

This paper is in a collection of

**“Historic Publications in Electrochemistry”**

which is part of

**Electrochemical Science and Technology Information  
Resource (ESTIR)**

(<http://electrochem.cwru.edu/estir/>)

APRIL 1965

VOL 112 • NO. 4

## EDITORIAL

C. V. King  
... 102C  
The World Needs Truth and Honesty

## TECHNICAL PAPERS

E. M. Otto  
... 367  
Equilibrium Pressures of Oxygen over  $MnO_2$ - $Mn_2O_3$  at Various Temperatures

E. J. Casey,  
A. R. Dubois,  
P. E. Lake, and  
W. J. Moroz  
... 371  
Effects of Foreign Ions on Nickel Hydroxide-Cadmium Electrodes

K. Fueki and  
J. B. Wagner, Jr.  
... 384  
Studies of the Oxidation of Nickel in the Temperature Range of 900 to 1400°C

J. C. Banter  
... 388  
Determination of the Refractive Index and Thickness of Oxide Films on Anodized Zirconium from Interference Measurements

J. J. Melchiorre and  
I. W. Mills  
... 390  
The Role of Copper during the Oxidation of Transformer Oils

R. Dreiner,  
K. Lehovc, and  
J. Schimmel  
... 395  
Growth Mechanism of Thin Anodic Oxide Films on Tantalum

A. H. Graham,  
R. W. Lindsay, and  
H. J. Read  
... 401  
The Structure and Mechanical Properties of Electroless Nickel

J. B. Kushner  
... 413  
Relationship between Deposit Thickness and Density during the Early Stages of Electrodeposition

R. S. Zucker  
... 417  
Growth of Single Crystal Cuprous Oxide from Melt and Luminescence of Cuprous Oxide

E. J. Mets  
... 420  
Poisoning and Gettering Effects in Silicon Junctions

M. Rubenstein  
... 426  
The Preparation of Homogeneous and Reproducible Solid Solutions of GaP-GaAs

B. E. Deal and  
M. Sklar  
... 430  
Thermal Oxidation of Heavily Doped Silicon

K. Tung  
... 436

The Effects of Substrate Orientation on Growth

Sekine,  
Yamura, and  
Sugino  
... 439

Mechanism of Hydrocarbon Formation in Electrolytic Reduction of Acetone in Aqueous Acid

Hellbardt  
... 443

Transpiration in an Open Tube GaAs/Al/Al<sub>2</sub>O<sub>3</sub>/H<sub>2</sub>

B. Tankins,  
F. Erthal, and  
K. Thomas, Jr.  
... 446

The Thermodynamic Properties of Dilute Solutions of Oxygen in the Liquid Binary Cu-Ni Alloy

R. Will  
... 451

Hydrogen Adsorption on Platinum Single-Crystal Electrodes, I. Isotherms and Heats of Adsorption

## TECHNICAL NOTES

Chiola and  
A. Vanderpool  
... 456

The Preparation and Luminescence of Monoclinic Phosphate

Bergh  
... 457

The Correlation between Water Contact Angle and KPR Adherence on SiO<sub>2</sub> Surfaces

Sosenberg,  
Kozlowski,  
McAleer, and  
Pollak  
... 459

Strain Patterns in GaS<sub>(1-x)</sub>P<sub>(x)</sub> Alloy Overlayers

Woolley  
... 461

Thermal Expansion of GaSb at High Temperatures

Schman and  
Hockings  
... 461

The Heats of Fusion of InSb, InAs, GaAs, and AlSb

## LETTERS OF COMMUNICATION

Fraser and  
Barradas  
... 462

A Simplified Calculation of Tafel Slopes for Successive Electrochemical Reactions

## ANNOUNCEMENT AFFAIRS

... 462-112C

# Hydrogen Adsorption on Platinum Single Crystal Electrodes

## I. Isotherms and Heats of Adsorption

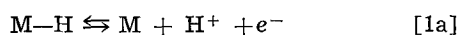
Fritz G. Will

Research Laboratory, General Electric Company, Schenectady, New York

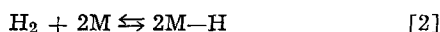
### ABSTRACT

The adsorption of hydrogen on the three main faces (100), (111), and (110) of platinum single crystal electrodes has been studied in 8N H<sub>2</sub>SO<sub>4</sub> at different temperatures with the voltage sweep method. As on polycrystalline platinum electrodes, hydrogen adsorbs on each of the faces in two distinctly different binding states which present themselves as two pronounced maxima in the current-voltage sweep curves. There are indications for a third binding state giving rise to a third, less pronounced maximum. The potentials at which the maxima occur are essentially the same for polycrystalline and for each of the three single crystal electrodes. However, the relative heights of the maxima are different in each case. The adsorption isotherms and the heats of adsorption are also notably different on the three faces. Under the usual assumption of one hydrogen atom adsorbed per platinum surface atom, initial roughness factors of 1.0-1.9 result which increase to 1.9-2.4 during the experiments. The results suggest that, in fact, each of the crystal faces exposes more than one crystal plane. The left pronounced maximum is assigned to a (110) plane, the right pronounced maximum to a (100) plane, and the third small maximum to a (111) plane. Different proportions of these planes determine the different shape of the curves obtained on the different nominal faces and on polycrystalline electrodes.

The adsorption of hydrogen on polycrystalline platinum electrodes has been studied extensively in the past. Three different methods are available for these studies, (a) charging curves (1), (b) polarization with an alternating current (2), and (c) polarization with a triangular voltage sweep (3) also referred to as cyclic voltammetry or surface coulometry. All these methods are based on the fact that a change of the electrode potential in a certain range causes a change of the coverage of the electrode surface with hydrogen atoms. The adsorption-desorption process occurs through the charge transfer reaction



in acid and alkaline solutions, respectively. For polarizations larger than about 50 mv, the charge transfer reaction [1] is much faster (4) than the dissociation-recombination reaction



Hence, for a given polarization, a certain coverage of the surface with hydrogen atoms is established and maintained by fast discharge of hydrogen ions or hydroxyl ions according to the discharge reaction [1].

The partial pressure of molecular hydrogen near the electrode surface which corresponds to that given polarization, on the other hand, is established much slower due to the slower rate of the dissociation reaction [2]. For any given polarization, the partial pressure of molecular hydrogen can be calculated from Nernst's law. At 0 volt (1 atm hydrogen pressure), the platinum surface is nearly saturated with hydrogen; at 0.4v ( $\approx 10^{-14}$  atm), the surface is essentially free of hydrogen. It can thus be seen that a change of the electrode potential has the same effect on the hydrogen coverage of the surface as a change of the partial pressure of molecular hydrogen. In contrast to the latter method, however, the first method does not depend on the slow dissociation equilibrium [2].

In general, adsorption isotherms obtained on "active" polycrystalline platinum electrodes with either of the three methods exhibit three inflection points. These manifest themselves in two waves in the charging curves (5-7), and in two distinct maxima and one minimum in the differential capacity curves (8,9) and in the current-voltage sweep curves (3,10). Figure 1 shows a typical curve obtained on polycrystalline platinum with the sweep method. Apparently, hydrogen adsorbs on platinum preferentially at two distinct voltages or hydrogen pressures, *i.e.*, hydrogen exists in a strongly and a weakly bound state. Increasing voltage corresponds to decreasing hydrogen pressure, and hence the left maximum corresponds to weakly bound hydrogen and the right maximum to strongly bound hydrogen. Little conclusive information is available about the nature of the two states of adsorption.

Slygin and Frumkin (6,11) measured the amounts of anions and cations which are adsorbed on platinum as a function of the potential. They found that these amounts are influenced notably by the adsorption of hydrogen and interpret (12) their results as the adsorption of negatively polarized hydrogen at larger potentials (small coverages) followed by the adsorption of positively polarized hydrogen at smaller potentials (large coverages). Wicke and Weblus (8) found that the right maximum is influenced by the nature of the anions in the electrolyte while the left maximum does not show such a dependence. From this Eucken and Weblus (8) believe that the two maxima are not due to adsorption on two different crystallographic planes of the platinum but are due to adsorption on bare platinum (right maximum) and on oxygen atoms (left

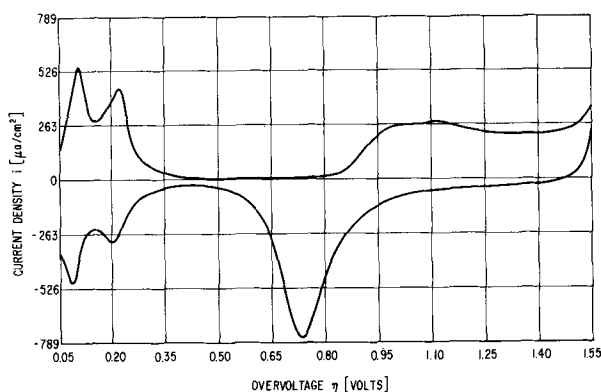


Fig. 1. Current-voltage sweep curve on polycrystalline platinum, obtained earlier (3). Sweep range 50-1550 mv, sweep rate 0.1 v/sec; surface area of electrode 0.19 cm<sup>2</sup>.

maximum). Böld and Breiter (13) found values for the heat of adsorption of hydrogen on platinum in excess of 10 kcal/mole  $H_2$  for coverages smaller than 0.5. This indicates that the strongly bound hydrogen is adsorbed as atoms. Kinetic considerations lead Breiter (14) to believe that the weakly bound hydrogen is also adsorbed as atoms.

Studies of hydrogen adsorption on platinum in the gas phase have also revealed the existence of strongly and weakly bonded hydrogen. Disagreement exists concerning the polarity of the two types of hydrogen and whether the weakly bound hydrogen is adsorbed as atoms or as molecules. Mignolet (15) measured the changes in the work function of a clean platinum film, which occur as a function of time, when hydrogen is being adsorbed at  $-190^\circ C$ . Using both the condenser and the thermionic method, he found that the first 40% of the hydrogen which adsorbs increases the work function by 0.11v while the remaining 60% decreases the work function of the clean metal by 0.23v. At  $20^\circ C$ , under vacuum, only the initial 40% hydrogen which increases the work function remains adsorbed. These findings suggest that the initially adsorbed hydrogen is strongly bonded and negatively polarized and the subsequent 60% hydrogen weakly adsorbed and positively polarized. Mignolet also found that a volume of carbon monoxide almost equal to that of the weakly bonded hydrogen could be adsorbed in addition to the strongly bonded hydrogen. From this he believes that the weakly bonded hydrogen is adsorbed as molecules. It has been shown (16), however, that carbon monoxide displaces the weakly and strongly bonded hydrogen from the surface. Hence, the foregoing contention does not seem to be valid. Rootsaert *et al.* (17) adsorbed and desorbed hydrogen on a platinum tip in a field emission microscope by changing the temperature at a constant hydrogen pressure of  $10^{-7}$  mm Hg. They found in agreement with Mignolet that on adsorbing hydrogen the work function first increases, passes through a maximum at a coverage of about 0.4, and then decreases with further increasing coverage. Pliskin and Eischens (18) obtained two absorption bands in infrared spectra of hydrogen adsorbed on alumina-supported platinum. When working with hydrogen and deuterium mixtures, they could not find any band corresponding to  $H - D^+$  bonds. From this they deduce that the weakly bonded "positive" hydrogen is not adsorbed as molecules. Toya (19) showed that the two absorption bands correspond to a difference in heats of adsorption of only 0.8 kcal/mole  $H_2$ . This small difference makes it unlikely that the strongly and weakly bonded hydrogen discussed earlier is identical with the two types causing the two absorption bands. For the former, differences in heat of adsorption are found (10,20) which are of the order of 8 kcal/mole  $H_2$ .

The following study was undertaken to find out more about the nature of the two states of hydrogen adsorption. In particular, this study is concerned with the question whether the two states are due to adsorption on two different crystallographic planes preferentially exposed by the polycrystalline platinum. In order to test this possibility, the adsorption of hydrogen on the three main faces (100), (111), and (110) of platinum single crystals was studied. The voltage sweep method was applied because it affords a convenient and accurate way to determine the quantities of adsorbed hydrogen (3).

### Experimental

The platinum single crystal was obtained by zone melting a platinum rod of 99.999% original purity in an electron beam. After orientation the crystal was cut with a diamond cutting wheel to give single crystals presenting the main faces (100), (111), and (110). These faces were then polished to optical flatness using for the final finish a  $0.1\mu$  alumina powder. The three single crystals were subsequently annealed in vacuum at  $680^\circ C$  for 24 hr and finally sealed into lime glass so that only the three faces of interest remained uncov-

ered. The geometric surface areas were  $0.181\text{ cm}^2$  for (100),  $0.328\text{ cm}^2$  for (111), and  $0.225\text{ cm}^2$  for (110). The three crystals were symmetrically arranged in one cell compartment opposite the counter electrode. A hydrogen reference electrode was located in a second cell compartment which communicated with the main compartment via a capillary. All potentials are referred to this hydrogen electrode. The 8N  $H_2SO_4$  used in the experiments was prepared with ultrapure water (21) and pre-electrolyzed for 15 hr. Although the measurements were carried out without gas-bubbling, the electrolyte was periodically flushed with prepurified argon to remove traces of hydrogen and oxygen.

Despite the cleaning procedures, reproducible results could be obtained only by applying a periodic sweep of such an amplitude that an oxide layer was formed and reduced during each sweep (compare Fig. 1) prior to the adsorption and desorption of the hydrogen layer. A sweep range of 50-1550 mv was chosen to achieve this and at the same time, hold the formation of molecular hydrogen and oxygen to a minimum. The applied sweep rate was 0.1 v/sec and, hence, the duration of one sweep was 30 sec. A modified (22) Hewlett Packard Function Generator 202A in conjunction with a potentiostat was used to apply the voltage sweeps. The resulting current-voltage (or time) curves were displayed on a Tektronix 502 x-y oscilloscope. For each face and each given temperature, photographs were taken of the first four sweeps and every 5 min thereafter for 20 min. A 35 mm "ROBOT" automatic transport and rewind camera was used for this purpose. The integration of the enlarged curves was performed graphically with an "Ott" planimeter No. 144 to a precision of 2%. Measurements on the three crystal faces were made at  $0^\circ$ ,  $10^\circ$ ,  $25^\circ$ ,  $40^\circ$ ,  $60^\circ$ , and  $80^\circ C$ . A specially designed circulating air thermostat allowed the temperature to be controlled within  $\pm 0.1^\circ C$ .

While one particular face was being studied, the other two faces were kept in the solution on open circuit. When proceeding to the next face, a potential of 50 mv was always applied for 3 min before starting the periodic sweep from this potential. During the experiments which are reported here, each face was subjected to some 240 sweeps. In preceding preliminary experiments, about 160 sweeps had already been applied to each individual face.

### Results

*Current-voltage sweep curves.*—As mentioned before, hydrogen desorbs from polycrystalline platinum electrodes preferentially at two different potentials corresponding to two distinct maxima in the current-voltage sweep curve. Figure 1 shows one such curve which was previously (3) obtained on polycrystalline platinum wires under conditions similar to those in the present study. The ratio of the currents of the "first" (less anodic) and "second" maximum  $I_1/I_2$  is 1.2. Figure 2 shows curves which were obtained on the (100), (111), and (110) faces of platinum single crystals at  $25^\circ C$ . The curves correspond to sweep 260 and were photographed 10 min after starting the periodic sweep. The two striking features of the curves for (100) and (111) are: (a) as on a polycrystalline electrode there are still two distinct desorption maxima, and (b) while for the (100) face the first maximum is smaller than the second, the opposite is true for the (111) face; in fact the ratio  $I_1/I_2$  is 0.8 for (100) and 1.5 for (111). The curve for the (111) face exhibits a small third maximum which degenerates to a shoulder in the curve for the (100) face. The curve obtained on the (110) face looks strikingly similar to the curve for (111), and the ratio  $I_1/I_2$  is essentially the same for the two faces. However, the current densities  $i_1$  and  $i_2$  corresponding to the two maxima of the (110) curve are some 30% smaller than  $i_1$  and  $i_2$  for (111).

The effect of temperature on the curves is such that with increasing temperature the height of the maxima increases and their position is shifted toward less anodic

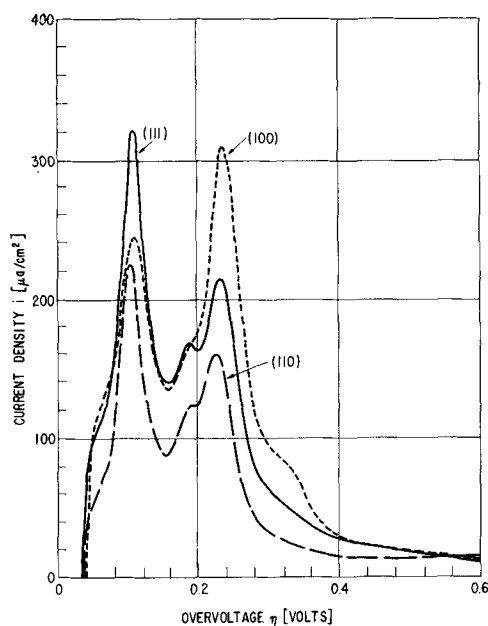


Fig. 2. Current-voltage sweep curves on platinum single crystal faces (100), (111), and (110) at 25°C. Sweep range 50-1550 mv, sweep rate 0.1 v/sec.

potentials. Both effects are larger for the first maximum.

During the 20-min duration of one experiment, the shape of the curves from the fourth sweep on remained essentially unaltered. The first curve and, to much lesser extent, the second and third curve always looked quite different from the succeeding curves.

The effect of the number of sweeps on the shape of the curves was quite pronounced, however, during the first 20 or 30 sweeps that were applied to the virgin crystal faces. Figure 3 shows this effect for the (110) face, where it is most pronounced. Curve I resulted when the 10th sweep was applied to the virgin surface. Curve II is identical to the (110) curve in Fig. 2 and was obtained after about 250 sweeps had been applied to the (110) face. While maximum 1 did not change too much, maximum 2 increased considerably with increasing number of sweeps. In fact, maximum 2 is smaller than maximum 3. After 10 sweeps, the ratio of the maxima currents  $I_1/I_2$  is 2.9, and after 260 sweeps this ratio is 1.45. The corresponding figures for the (111) face are 2.1 (10 sweeps) and 1.5 (260 sweeps) and for the (100) face 0.79 and 0.80.

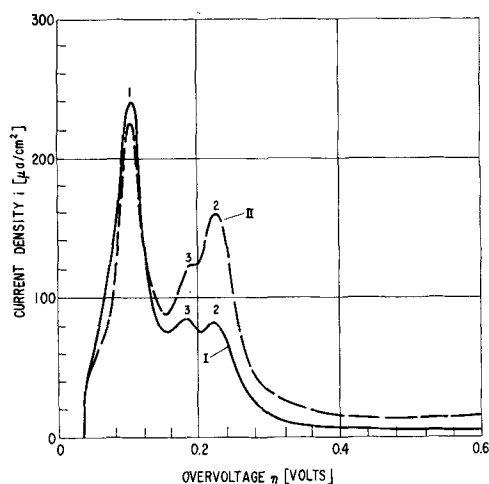


Fig. 3. Current-voltage sweep curves on the (110) face at 25°C after 10 sweeps (curve I) and after 260 sweeps (curve II).

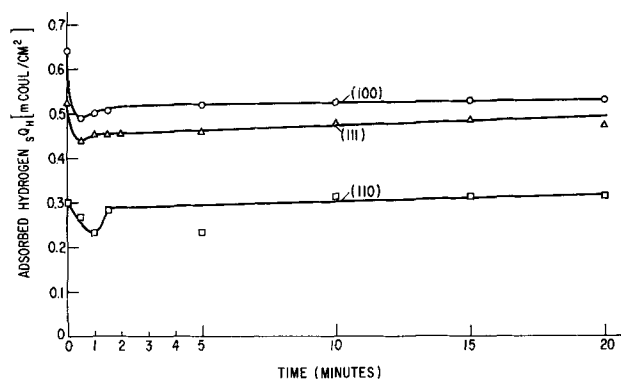


Fig. 4. Saturation amounts of hydrogen adsorbed on the three faces at 25°C.

*Saturation concentration of adsorbed hydrogen.*—Since a voltage is applied which changes linearly with time, the current-voltage curves in Fig. 1 and 2 also represent current-time curves. Hence, an integration of these curves yields the charge corresponding to the amount of adsorbed hydrogen plus the charge of the double layer capacity. The double layer capacity is almost constant between 50 and 400 mv (11). Its charge is only about 2% of the charge of adsorbed hydrogen and shall be neglected. The small current above potentials of about 400 mv is mostly due to the charge of the double layer (3). Below 50 mv the current decreases steeply. Therefore, the saturation concentration of hydrogen  $sQ_H$  adsorbed on the surface can be determined by integrating the curves from 50 to 400 mv. This was done for different times in the temperature range of 0° to 80°C. The result at 25°C for sweeps 240 to 280 is plotted in Fig. 4. During the first two or three sweeps of each experiment, erratic values are found for  $sQ_H$ . From then on,  $sQ_H$  changes but slightly with time. This finding agrees with the finding concerning the changes in the shape of the curves with time.

For the first 10 sweeps that were applied to the virgin faces, considerably smaller amounts of hydrogen were found. The  $sQ_H$  values for 10 sweeps are 0.39 mCoul/cm<sup>2</sup> for (100), 0.23 for (111) and 0.24 for (110).<sup>1</sup> The corresponding values after 260 sweeps are 0.51 mCoul/cm<sup>2</sup> for (100), 0.46 for (111), and 0.30 for (110).

For the first sweep of each experiment, the total anodic charge, i.e., adsorbed hydrogen plus oxygen, is always between 14% and 34% larger than the total cathodic charge. However, for the succeeding sweeps, the total anodic charge is consistently smaller than the cathodic charge, namely, by 1 to 12%.

Except for the (110) face, temperature has no systematic effect on the  $sQ_H$  values. For the (110) face,  $sQ_H$  stays roughly constant between 0° and 40°C and then decreases by about 20% from 40° to 80°C.

*Adsorption isotherms.*—The sweep curves obtained after 10 min for different temperatures were integrated in intervals of 50 mv between 50 and 400 mv. The degree of coverage  $\theta = Q_H/sQ_H$  at, e.g., 300 mv, is the ratio of the charges resulting from an integration between 400 mv and, e.g., 300 mv, and between 400 mv and 50 mv. The resulting adsorption isotherms for the (100) face are presented in Fig. 5. Applying Nernst's law and correcting for the vapor pressure of the sulfuric acid, the overvoltages are converted into partial pressures of molecular hydrogen. As one would expect for an exothermic process, the degree of coverage decreases with decreasing hydrogen pressure and increasing temperature. The curves display three inflection points in accordance with the three extrema

<sup>1</sup> Note added during revision of manuscript: According to a private communication on October 12, 1964, Dr. J. E. Oxley, Leeson Moos Laboratory, in similar experiments on Pt single crystals obtained  $sQ_H$  values of 0.30 mCoul/cm<sup>2</sup> for (100), 0.29 for (100), and 0.21 for (110). The results were obtained at a sweep rate of 18 v/sec.

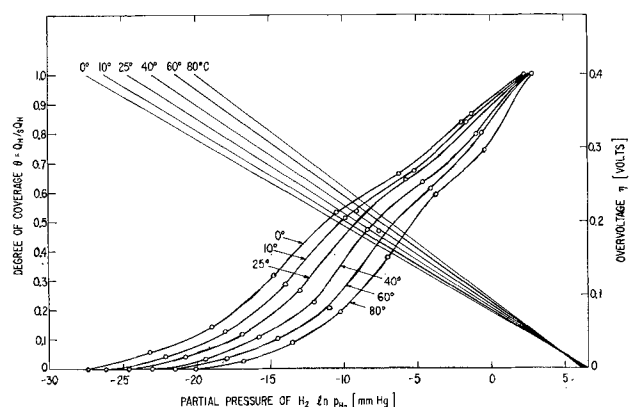


Fig. 5. Adsorption isotherms on (100) face. Straight lines relate voltage on right ordinate to partial pressure of hydrogen.

of the current-voltage sweep curves. Figure 6 shows the adsorption isotherms for the three crystal faces at 0° and 80°C. For constant hydrogen pressure, the degree of coverage decreases distinctly in the whole temperature range in the order (100) > (111) > (110). The effect is more pronounced at lower temperatures.

**Heats of adsorption.**—The Clausius-Clapeyron equation

$$dp/dT = \Delta H/T\Delta V \quad [3]$$

( $\Delta H$ ,  $\Delta V$  enthalpy and volume change on transferring 1 mole of hydrogen from the gas phase into the adsorbed phase) may be written as

$$d \ln p_{H_2}/dT = W/RT^2 \quad [4]$$

if one assumes ideal conditions in the gas phase and neglects the volume of the hydrogen in the adsorbed phase. The heat of adsorption  $W \equiv \Delta H$  is negative for an exothermic process. If the heat of adsorption is temperature independent the integration of equation [4] gives

$$\ln p_{H_2} = -W/RT + \text{const.} \quad [5]$$

In a plot  $\ln p_{H_2}$  against  $1/T$  straight lines should result whose slope is proportional to the heat of adsorption (10, 13). While this is indeed the case for the (100) and (111) faces, the heat of adsorption increases noticeably with increasing temperature for the (110) face at temperatures above 40°C.

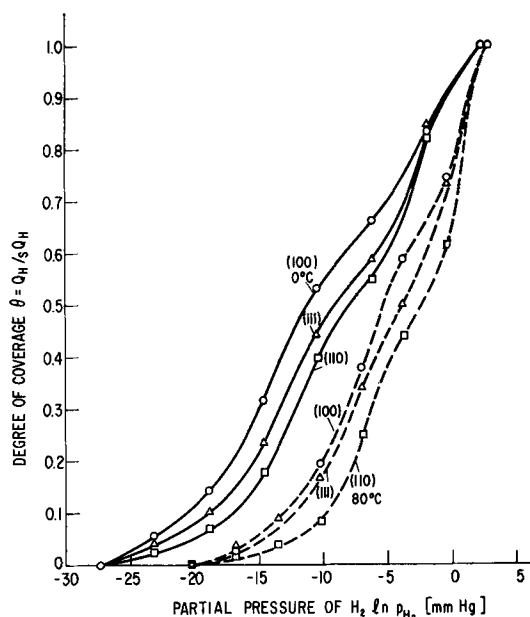


Fig. 6. Adsorption isotherms on (100), (111), and (110) at 0° and 80°C.

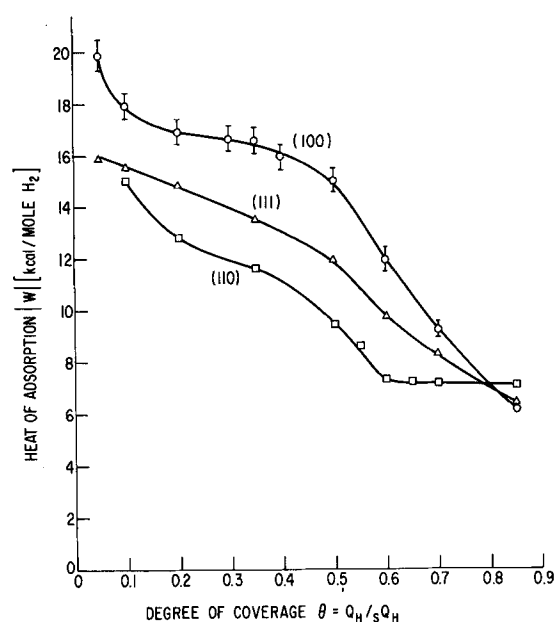


Fig. 7. Heats of adsorption of hydrogen on the three crystal faces as a function of coverage.

The heats of adsorption for the three crystal faces are plotted in Fig. 7 as a function of the degree of coverage. For the (110) face the temperature-independent values of  $W$  between 0° and 40°C are shown. For all three crystal faces, the heat of adsorption decreases substantially with increasing coverage. This agrees with results obtained on polycrystalline platinum in electrolytes (10, 13) and in the gas phase (20). Especially in the curve for the (110) face one can clearly distinguish between strongly and weakly bonded hydrogen; the latter prevails at  $\theta > 0.6$  and has a heat of adsorption of about 7 kcal/mole. An increase of  $\theta$  from 0.1 to 0.85 causes a decrease in the heat of adsorption of 66% for (100), 59% for (111), and 53% for (110). The other noteworthy finding is the comparatively large difference in the heats of adsorption for the different faces. Except for coverages larger than 0.8 the heats of adsorption decrease in the order (100) > (111) > (110). At coverages larger than 0.8, near saturation, this order is reversed. For coverages smaller than 0.6 the difference in  $W$  between the three faces averages between 2 and 3 kcal. For  $\theta = 0.5$  the heats of adsorption are 15 kcal/mole  $H_2$  for (100), 11.9 for (111), and 9.4 for (110).

## Discussion

**Roughness of the surface.**—The number of platinum atoms in the surface planes of the three crystal faces are  $1.5 \cdot 10^{15}$  atoms/cm<sup>2</sup> for (111),  $1.3 \cdot 10^{15}$  for (100), and  $0.92 \cdot 10^{15}$  for (110). If one makes the usual assumption that one hydrogen atom is adsorbed per platinum surface atom, the corresponding charges are 0.24 mCoul/cm<sup>2</sup> for (111), 0.208 for (100), and 0.147 for (110). The amounts of hydrogen that are found are considerably larger, particularly after the faces have been subjected to a large number of sweeps. This may be interpreted as a large initial roughness of the virgin faces which further increases with the number of sweeps applied. For the (100) face, for example, the roughness factor would be 1.87 after 10 sweeps and 2.45 after 260 sweeps. With such a large surface roughness, it is probable that the surface exposes more than one crystal face. The fact that the current maxima on all three faces occur to within  $\pm 5$  mv at the same potentials (compare Fig. 2) could indicate that each of the faces is, in truth, a mixture of essentially two faces with a small fraction of a third face, particularly in the case of the nominal (111) and (110) face.

**Effect of sweep on curve shape.**—The effect of the number of sweeps on the shape of the curves (com-

pare Fig. 3) might be explained as follows. Initially (curve I), the nominal (110) face exposes a large fraction of (110) (maximum 1) and small fractions of (111) (maximum 3) and of (100) (maximum 2). After 260 sweeps have been applied (curve II), the amount of (110) has decreased slightly, the fraction of (111) stayed almost constant, but the fraction of (100) increased sharply. The periodic voltage sweep might cause the formation of etch pits with the exposure of preferred crystal faces. In this connection, it is interesting to note that the development of low-index planes by chemical etching is a standard technique in the determination of the orientation of various metal crystals (23).

The curve obtained on the (111) face (compare Fig. 2) looks always quite similar to that on the (110) face. This implies that the nominal (111) face exposes, in fact, always a large fraction of (110) (maximum 1), a considerable fraction of (100) and only a small fraction of (111). In order to rationalize this conclusion one has to assume that a thin surface layer exhibits a polishing and recrystallization texture which exposes the preferred orientations that are found. Indeed, a preferred orientation has been found on cold rolled and of polished copper and gold, with (110) planes lying parallel to the surface (24). The recrystallization texture on annealing may or may not resemble the polishing texture, depending on the severity of the surface damage and the particular annealing conditions (23). As mentioned before, the platinum crystals were annealed at 680°C for 24 hr. On platinum single crystals that had been annealed at 1100°C for 48 hr, Tucker (25) did not find evidence for faceting. However, the detection of crystal facets smaller than about 100Å in diameter is beyond the sensitivity of the slow electron diffraction apparatus.

*Adsorption isotherms and heats of adsorption.*—In the preceding discussion, maximum 1 has been assigned to a (110) plane, maximum 2 to a (100) plane, and maximum 3 to a (111) plane. This assignment is based on the relative heights of the current maxima for the different nominal faces in Fig. 2. It implies that the hydrogen bond is weakest on the (110) plane and strongest on the (100) plane. This agrees with the heats of adsorption for the three faces shown in Fig. 7, which increase in the order  $(110) < (111) < (100)$  for coverages smaller than 0.8. Based on considerations involving the number of nearest neighbors and their degrees of unsaturation, one would argue, however, that the bond should be weakest on the (111) plane and strongest on the (110) plane. More experiments are needed to solve this apparent contradiction.

Qualitatively, the different adsorption isotherms for the different faces can be understood with the proposed assignment of the current maxima. Since, for example, the nominal (110) face exposes a much smaller surface fraction of (100) than the nominal (100) face, it is evident that at smaller partial pressures of hydrogen, where (100) adsorbs preferentially, the surface coverage is smaller for the nominal (110) face than for the nominal (100) face. On a similar basis, the difference in heats of adsorption can be understood.

*Current-voltage curves on polycrystalline wires.*—The two pronounced maxima of current voltage curves obtained on polycrystalline platinum wires (compare Fig. 1) occur at essentially the same potentials as those obtained on the single crystal faces. The texture of cold-drawn wires of face-centered cubic metals, like platinum, is usually a double fiber texture with a [111] and a [100] direction parallel to the wire axis (23). With the possibility of so many different crystal planes exposed it seems surprising that only two maxima are observed. This difficulty can be reconciled by postulating that the wire surface becomes etched in the usual pretreatments of the electrodes prior to the experiments. In this etching process, the low-energy main faces are expected to develop at the expense of the large number of high-index planes.

## Conclusions

The finding that the maxima have different heights for the different faces, but occur at almost the same potentials, suggests that each of the nominal faces exposes, in fact, several crystal planes in different proportions. Such an interpretation is consistent with the assumption that the large measured amounts of adsorbed hydrogen are due to a considerable surface roughness. The left pronounced maximum has been tentatively assigned to a (110) plane, the right pronounced maximum to a (100) plane and the third small maximum to a (111) plane. This implies that the bond strength of hydrogen and, hence, its heat of adsorption is smallest on (110) and largest on (100). This has been actually found. The two adsorption states of hydrogen that exist on polycrystalline platinum electrodes are also likely to be due to adsorption of hydrogen on two different crystallographic planes. The two current maxima occur within  $\pm 5$  mv at the same potentials as the two pronounced maxima on the single crystals. Hence, it is concluded that cold-worked, polycrystalline platinum electrodes expose mainly crystallites with {110} and {100} planes. This conclusion is in agreement with the fact that the texture of all cold-rolled face-centered cubic metals is one in which {110} planes are parallel to the rolling plane (23). To reconcile the occurrence of only two or three current maxima on cold-drawn platinum wires with their texture of [111] and [100] parallel to the axis, one has to assume etching of the surface during the process of "activating" the electrodes. Studies with better defined crystal planes and under extreme clean conditions are needed to confirm these tentative conclusions.

## Acknowledgments

The author gratefully acknowledges the loan of the platinum single crystals by C. W. Tucker which were prepared by J. W. Rutter and V. J. DeCarlo.

Manuscript received July 20, 1964. This paper was presented at the Toronto Meeting, May 3 to 7, 1964.

Any discussion of this paper will appear in a Discussion Section to be published in the December 1965 JOURNAL.

## REFERENCES

1. F. P. Bowden, *Proc. Roy. Soc.*, **A125**, 446 (1929).
2. P. Dolin and B. Ershler, *Acta physicochim. URSS*, **13**, 747 (1940).
3. F. G. Will and C. A. Knorr, *Internat. Polarograph. Kolloqu.*, Bonn 1958; *Z. Analyt. Chem.*, **173**, 87 (1960); *Z. Elektrochem.*, **63**, 1008 (1959); *ibid.*, **64**, 258 (1960).
4. J. Giner, *Z. Elektrochem.*, **63**, 386 (1959).
5. J. A. V. Butler and G. Armstrong, *Proc. Roy. Soc.*, **A137**, 604 (1932).
6. A. Slygin and A. Frumkin, *Acta physicochim. URSS*, **3**, 791 (1935).
7. M. Breiter, C. A. Knorr, and W. Völkl, *Z. Elektrochem.*, **59**, 681 (1955).
8. A. Eucken and B. Weblus, *ibid.*, **55**, 114 (1951); E. Wicke and B. Weblus, *ibid.*, **56**, 169 (1952).
9. M. Breiter, H. Kammermaier, and C. A. Knorr, *ibid.*, **60**, 37 (1956).
10. M. Breiter and B. Kennel, *ibid.*, **64**, 1180 (1960).
11. A. Slygin, A. Frumkin, and W. Medvedovsky, *Acta physicochim. URSS*, **4**, 911 (1936).
12. A. Frumkin and A. Slygin, *ibid.*, **6**, 819 (1936).
13. W. Böld and M. Breiter, *Z. Elektrochem.*, **64**, 897 (1960).
14. M. Breiter, *Electrochim. Acta*, **7**, 25 (1962).
15. J. C. P. Mignolet, *J. Chim. Phys.*, **54**, 19 (1957).
16. S. Gilman, *J. Phys. Chem.*, **67**, 78 (1963).
17. W. J. M. Rootsart, L. L. Van Reijen, and W. M. H. Sachtler, *J. Catalysis*, **1**, 416 (1962).
18. W. A. Pliskin and R. P. Eischens, *Z. phys. Chem. N. F.*, **24**, 11 (1960).
19. T. Toya, *J. Res. Inst. Catalysis* (Hokkaido University), **10**, 236 (1962).
20. J. G. Aston, *J. Phys. Chem.*, **67**, 2042 (1963).
21. R. W. Powers, *Electrochem. Technol.*, **2**, 274 (1964).
22. F. G. Will, To be published.
23. C. S. Barrett, "Structure of Metals," McGraw-Hill Book Co., New York (1952).
24. C. S. Lees, *Trans. Faraday Soc.*, **31**, 1102 (1935).
25. C. W. Tucker, *J. Appl. Phys.*, **35**, 1897 (1964).